Structural, Electrical and Magnetic Properties of $SrCo_xFe_{12-x}O_{19}$ ($0\leq x \leq 1$) Prepared by Co-precipitation Method

Deepti V. Ruikar[1], P.B. Kashid[2], S. Supugade[3], N. Pisal[4], Vijaya Puri*[5]

[1]Department of Basic Sciences and Humanities, Bharati Vidyapeeth College of Engineering, Kolhapur, Maharashtra, India

[2, 3, 4, 5]Thick and Thin Film Device Lab., Department of Physics, Shivaji University Kolhapur, Maharashtra, India

[1]deeptikulkar@yahoo.com; *[5]vrp_phy@unishivaji.ac.in

Abstract

Single phase Cobalt doped strontium hexaferrite with chemical formula $SrCo_xFe_{12-x}O_{19}$ ($0\leq x \leq 1$) has been prepared by the chemical co-precipitation technique. The crystallite size of the samples is in the range of 32–55 nm. The density and uniformity of particle size distribution rose with the increase in cobalt concentration. The DC resistivity, Curie temperature, activation energy and charge carrier concentration of the $SrCo_xFe_{12-x}O_{19}$ discs were studied. The DC resistivity of the strontium hexaferrite was increased due to cobalt doping. Doping with Co^{2+} is found to considerably affect the lattice *c*-parameter, crystallite size (D), Curie temperature (T_C), DC resistivity (ϱ) and drift mobility (μ_d). Synthesized samples possessed excellent electrical and magnetic properties applicable in microwave devices.

Keywords

Magnetic Oxides; Chemical Synthesis; Precipitation; Crystal Structure; Electrical Properties; Magnetic Properties

Introduction

Ferrites, a large class of oxides with remarkable magnetic properties, have been investigated and applied during the last ~50 years (R.Venezuela et al.). Hexaferrites have attracted special attention due to their interesting electrical and magnetic properties. Polycrystalline hexagonal ferrites have technological importance in different fields, such as microwave devices, high-speed recording media, ferrofluids, catalysis and magnetic refrigeration systems (P.A. Shaikh et. al.; A. Haq et.al.). These materials are considered superior to other magnetic materials because of low eddy current losses (B.P. Rao et al.). Moreover, the magnetic and electrical properties of the hexaferrites can be tailored to specific device applications by the choice of the cation type and cation distribution between interstitial sites. The structural, electrical and magnetic properties of M type hexaferrite can be tailored by varying synthesis conditions as well as by doping divalent metal ion. Usually, there are two different ways to modulate the magnetic properties of barium ferrite, doping at Fe^{3+} sites and at Sr^{2+} sites. As substituting at Fe^{3+} sites, some different types of cationic combinations can be utilized including Co–Ti, La–Ti, Co–Sn, Ni–Zr, etc. (M.R. Eraky et al., M. J. Iqbal et al., S. Nilpairach et al. M. W. Pieper et al.).

The preparation techniques as well as the structural doping of Co ions influence the magneto-dielectric properties of this compound (P. Shepherd et al.). The experimental measurements for electric conduction, charge carrier concentration, charge carrier mobility and activation energy give much information on the behavior of the free and localized charge carriers. These systematic information leads to good explanation and understanding of the conduction mechanism in the studied hexagonal ferrite system. To the author's knowledge, there are reports on the highly cobalt doped $SrFe_{12}O_{19}$ with high level of doping; but rare reports are made on the stoichiometric composition series (low doping level) as reported in this paper (K. K. Mallick et al., H.A. Elkady et al.). The aim of this work is to show the effect of the composition on the conduction and magnetization mechanism for polycrystalline system $SrCo_xFe_{12-x}O_{19}$ prepared by co-precipitation technique.

Experimental Techniques

The series of cobalt doped strontium hexaferrite powders with chemical formula $SrCo_xFe_{12-x}O_{19}$ were

synthesized by chemical co-precipitation technique. The starting materials were chlorides as $SrCl_2.6H_2O$, $FeCl_3.6H_2O$ and $CoCl_2.6H_2O$. NaOH and Na_2CO_3 solution was used as base solution. The molar ratio of Fe/Sr was 12:1. The Weighed starting materials in stoichiometric amount were dissolved in distilled water; Na_2CO_3 and NaOH were taken in 1:4 ratio and dissolved in distilled water in order to obtain the base solution. The base solution ($NaOH/Na_2CO_3$) was added dropwise in Sr/Fe/Co solution along with stirring to get precipitate. Addition continued till solution with precipitate acquired desired pH of 11. The precipitate was washed by distilled water several times to remove NaCl traces and then filtered before. It was dried and pre-sintered at 450^{0}C. The synthesized $SrCo_xFe_{(12-x)}O_{19}$ powder was pressed to form disc shaped pellets with Polyvinyl Acetate as binder. The pellets were then sintered at 850^{o}C and this process was again repeated for different concentration of Fe and Co having stoichiometric formulae $SrFe_{12}O_{19}$, $SrCo_{0.1}Fe_{11.9}O_{19}$, $SrCo_{0.3}Fe_{11.7}O_{19}$, $SrCo_{0.5}Fe_{11.5}O_{19}$, $SrCo_{0.8}Fe_{11.2}O_{19}$ and $SrCoFe_{11}O_{19}$.

The studies on structural properties of the prepared samples were done by CrKα radiations using Philips X ray diffractometer (PW 3710) and Perkin Elmer-USA FTIR spectrometer and the surface morphology using JSM-JEOL 6360. DC electrical properties such as resistivity, activation energy, carrier concentration and Curie temperature of $SrCo_xFe_{(12-x)}O_{19}$ samples were studied by two probe method. The dc magnetic properties such as saturation magnetization, coercivity and remanent magnetization of these synthesized $SrCo_xFe_{(12-x)}O_{19}$ powders were measured by vibrating sample magnetometer (VSM Lakeshore 7307).

Results and Discussions

Structural Properties

The X ray diffraction pattern of the $SrCo_xFe_{12-x}O_{19}$ powders is shown in figure 1a and the magnified pattern to reveal the shift is shown in figure 1b. The hexagonal crystal system with dominant (107) plane was obtained for x=0, 0.1 and 1. The hexagonal crystal system with dominant (114) plane for x=0.3 and 0.5 whereas, dominant (201) plane was obtained for $SrCo_xFe_{12-x}O_{19}$ with x=0.8. The change in relative intensities due to variation in dopant concentration of the pattern may be related to the occupation of the different crystallographic sites of the crystal lattice. The (200) plane obtained for pure $SrFe_{12}O_{19}$ powder was totally suppressed due to Co^{2+} doping. From the magnified X ray diffraction pattern (fig. 1b), it was revealed that, the X ray diffraction peaks were shifted to the higher diffraction angle due to doping of Co^{2+} in place of Fe^{3+}. Quantitative information concerning the preferential crystallite orientation has been obtained from texture coefficient. TCs (hkl) was defined by relation (S. N. Mathad et al.),

$$TC\ (hkl) = \frac{\dfrac{I\,(hkl)}{I_0\,(hkl)}}{\dfrac{1}{N}\sum_N \dfrac{I\,(hkl)}{I_0\,(hkl)}} \quad \text{-------------(1)}$$

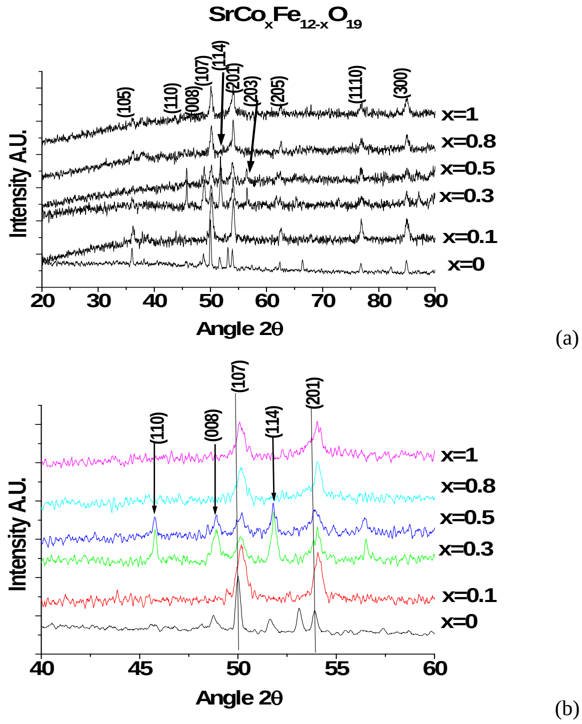

FIG. 1 X RAY DIFFRACTION PATTERN OF $SrCo_xFe_{12-x}O_{19}$ POWDER.

Where I (hkl) is the measured intensity, I_0 (hkl) is the ASTM intensity and N is the reflection number. The calculated texture coefficient (TC) of significant plane (hkl) is tabulated in Table 1.

The orientation of planes at (1110) is present in all the samples, which reveals that; the doping of Co fails to change the magnetoplumbite structure of $SrFe_{12}O_{19}$. However, the TC of (107) plane in pure strontium hexaferrite decreased due to cobalt doping in it which reveals that; for further higher Co^{2+} doping concentration, the hexagonal crystal system may get perturbed into the other. The calculated lattice parameters (a and c), cell volume, crystallite size and X ray density of the synthesized $SrCo_xFe_{12-x}O_{19}$ were calculated from the X ray diffraction data. The

crystallite size was calculated using the well known Debye Scherer's formula (K. K. Mallick et al.).

TABLE 1. TEXTURE COEFFICIENT OF $SrCo_xFe12\text{-}xO_{19}$

Composition (x)	Texture coefficient TC for significant (hkl) planes				
	(107)	(114)	(201)	(1110)	(300)
0	0.285	0.063	0.808	**2.467**	0.841
0.1	0.176	0.016	1.008	**3.659**	0.812
0.3	0.194	0.364	1.633	**2.734**	1.064
0.5	0.161	0.213	1.332	**4.499**	0.533
0.8	0.233	0.012	1.747	**2.446**	1.295
1	0.180	--	1.061	**2.566**	1.171

TABLE 2. STRUCTURAL PARAMETERS, CURIE TEMPERATURE OBTAINED BY ELECTRICAL CONDUCTIVITY AND MAGNETOCRYSTALLINE ANISOTROPY CONSTANT (K_1) OF $SrCo_xFe_{12\text{-}x}O_{19}$

Composition (x)	Lattice parameters A⁰		Crystallite size (nm)	X ray density ϱ (gm/cm³)	Curie temp. Tc (K)
	a	c			
0	5.881	23.072	55.15	2.552	496.18
0.1	5.868	22.990	39.11	2.573	683.29
0.3	5.870	22.912	48.87	2.582	632.25
0.5	5.848	22.989	32.58	2.594	622.94
0.8	5.867	21.940	48.88	2.703	632.25
1	5.871	21.646	41.391	2.738	642.45

The crystal axis ratio c/a as well as cell volume and crystallite size decreased due to Co^{2+} doping in $SrFe_{12}O_{19}$; which suggests the radius of crystal grains decreased resulting in increase in X ray density. The changes in the lattice constants occur due to the difference between ionic radii of dopants and the host ions. There are five positions of Fe^{3+} in the crystal lattice of magnetoplumbite ferrite 2a$\uparrow$, 2b$\uparrow$, 12k$\uparrow$, 4f1$\downarrow$ and 4f2$\downarrow$, where 4f1 is tetrahedral site, 2b is hexahedron site and 2a, 12k and 4f2 are octahedral sites [N. Chen et al.]. The Co^{2+} substitution of Fe^{3+} causes the shrinkage of crystal lattice, and the reason is the volume effect for which Co^{2+} with bigger radius must substitute Fe^{3+} in octahedral sites or probably that Co^{2+} substitution of Fe^{3+} causes the change in the crystal lattice binding energy. Consequently, the aberrance of the crystal lattice leads to the changes in the crystal lattice constants and the decrease of the radius of the crystal grains. This decrease in crystallite size is responsible for the shift in X ray diffraction peaks towards higher diffraction angle.

The Fourier transform Infrared absorption spectra of $SrCo_xFe_{12\text{-}x}O_{19}$ powder is shown in figure 2. The band at 578cm^{-1} is the characteristic band for Fe-O bond (W. Zhao et al.), which differing from those for γ-Fe_2O_3 is close to the E1u vibrations of Fe3-O bond in $SrFe_{12}O_{19}$. This indicated that γ-Fe_2O_3 of spinel ferrite had been transformed into hexaferrite skeletal. The band at 430 cm^{-1} has been assigned to A_{2u} vibrations of Fe4-O at 4f2 (octahedral) site; 540cm^{-1} to E_{1u} vibrations of Fe3–O at 4f1 (tetrahedral) site and 578cm^{-1} to E_{1u} vibrations of Fe3–O band at 4f1 (tetrahedral) site. Due to Cobalt doping; the absorption bands were shifted to the higher frequencies. The force constant of these bonds and bond radii of these bonds is tabulated in table 3.

As the ionic radius of Co^{2+} is more than that of Fe^{3+}; stretching of Fe4-O bonds may take place and hence the bond radii in $SrCo_xFe_{12\text{-}x}O_{19}$ increases due to Co^{2+} doping into $SrFe_{12}O_{19}$ and those of Fe3-O decreases which reveals that the IR absorption peaks of cobalt doped strontium hexaferrite are obtained due to stretching vibrations. Due to stretching of bonds, the higher the IR frequency is at which the bond will absorb cobalt doped strontium hexaferrites. Similarly, the IR absorption peaks get broadened due to doping of Co^{2+} in place of Fe^{3+} in $SrCo_xFe_{12\text{-}x}O_{19}$. The broadening of absorption band possible due to some oxygen atoms becomes more tightly bonded resulting in small positional disorder thus IR absorption will occur at varying frequencies (Doppler shifts) for each of these bonds. The end result is that the IR peak appears broadened as it is an average of all these slightly different absorptions.

Surface Morphology

The scanning electron microscopic images of $SrCo_xFe_{12\text{-}x}O_{19}$ discs is shown in figure 3. The pure strontium hexaferrite shows agglomerated hexagonal platelet like porous surface morphology. $SrCo_{0.1}Fe_{11.9}O_{19}$ discs formed with non-uniform agglomerated grains of size vary from 0.1μm to 1μm whereas, $SrCo_{0.3}Fe_{11.7}O_{19}$ discs show uniform, agglomerated granular surface morphology formed by grains of ~250nm. The $SrCo_xFe_{12\text{-}x}O_{19}$ discs with x increased from 0.5 to 1; and dense surface morphology with smaller grains were obtained. The $SrCo_{0.5}Fe_{11.5}O_{19}$ discs show the formation of nanoneedles along with agglomerated spherical grains of size of ~100 nm.

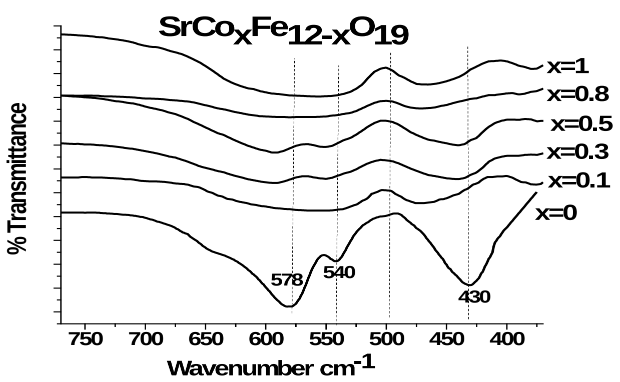

FIG. 2 FTIR ABSORPTION SPECTRA OF $SrCo_xFe_{12-x}O_{19}$.

TABLE 3. PARAMETERS FROM FTIR ABSORPTION SPECTRA

x	Force constant k N/m			Bond Radius r nm		
	432 cm^{-1} (Fe4-O)	540 cm^{-1} (Fe3-O)	578 cm^{-1} (Fe3-O)	432 cm^{-1} (Fe4-O)	540 cm^{-1} (Fe3-O)	578 cm^{-1} (Fe3-O)
0	135.6621	193.4795	237.2605	0.0219	0.0360	0.0257
0.1	166.2398	213.9482	282.4911	0.0254	0.0306	0.0230
0.3	152.5636	210.7903	299.1183	0.0238	0.0296	0.0195
0.5	151.5615	210.3973	285.6869	0.0239	0.0298	0.0222
0.8	152.2292	215.9338	280.6729	0.0247	0.0289	0.0250
1	152.5636	219.9325	296.7805	0.0248	0.0253	0.0243

The nanoneedles with width of 50nm and length of ~80nm were observed. The $SrCo_{0.8}Fe_{11.2}O_{19}$ and $SrCoFe_{11}O_{19}$ discs show dense granular surface of orbicular grains of size 60-70 nm and 40-50nm respectively. As cobalt content increased from 0 to 1; the grain size and porosity was reduced and density increased. This result agrees well with the crystallite size, cell volume and X ray density obtained from X ray diffraction studies. The doped strontium hexaferrite discs are much denser than the undoped one which resulta from that the dopant Co^{2+} ions fill into the gaps of the grains and increase the production of α-Fe_2O_3 in the course of pre-sintering to accelerate the building of $SrFe_{12}O_{19}$ crystals.

DC Electrical Properties:

The DC electrical resistivity of $SrCo_xFe_{12-x}O_{19}$ discs was measured by two probe method. The variation of resistivity of cobalt doped strontium hexaferrite discs with temperature is plotted in figure 4. The resistivity of pure $SrFe_{12}O_{19}$ discs is shown in inset of fig. 4. The Variation of Curie temperature with cobalt concentration (x) is tabulated in table 2. The resistivity and Curie temperature (Tc) of the pure strontium hexaferrite has been enhanced due to doping of Co^{2+} in place of Fe^{3+} ions. The $SrCo_xFe_{12-x}O_{19}$ show semiconducting behavior as the resistivity initially increased from room temperature ~30˚C upto certain temperature and decreased afterwards with increase in temperature. The behavior of initial increase in resistance with temperature and then decrease may be attributed to the spin canting. With the substitution and temperature variation, the spin canting angle changes are responsible for the initial increase in resistivity with temperature obtained (M. J. Iqbal et al.).

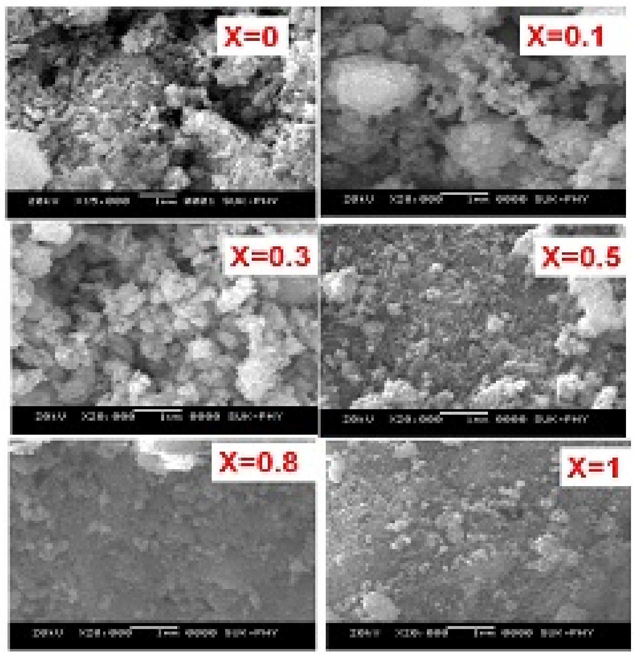

FIG. 3 SCANNING ELECTRON MICROSCOPIC IMAGES OF $SrCo_xFe_{12-x}O_{19}$ DISCS.

The electrical dc conductivity, σ_{dc}, in this region was fitted by Arhenius relation,

$$\sigma_{dc} = \sigma_0 \exp\left(\frac{-\Delta E}{k_B T}\right) \qquad \text{---------------(2)}$$

Where, σ_0 is the pre-exponential constant, T is the absolute temperature, k_B is the Boltzmann's constant and ΔE is the activation energy for electric conduction. The charge carrier concentration and activation energy calculated from the equations below is plotted with composition x as shown in fig. 5.

$$n = \frac{N_A \rho_m B}{M} \qquad \text{----------(3)}$$

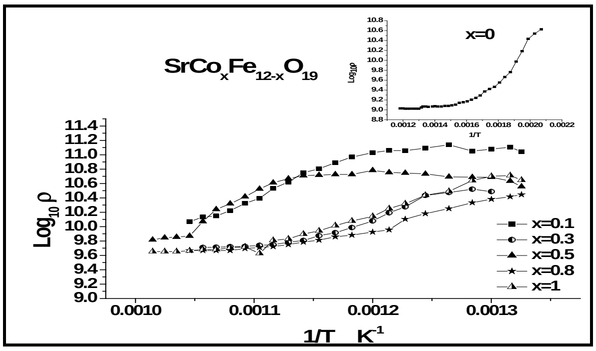

FIG. 4 VARIATION OF DC RESISTIVITY OF SRCOXFE12-XO19 DISCS WITH TEMPERATURE.

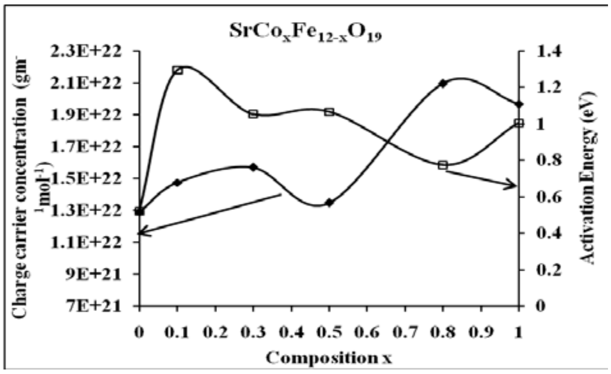

FIG. 5 VARIATION OF CHARGE CARRIER CONCENTRATION AND ACTIVATION ENERGY WITH COBALT CONCENTRATION (x) IN $SrCo_xFe_{12-x}O_{19}$ DISCS

where N_A is the Avogadro's number, ϱ_m is the measured density of sample, B is the number of iron atoms in the chemical formula of the materials and M is the molar mass of the sample.

DC Magnetic Properties

Figure 6 shows the DC magnetic hysteresis loops for $SrCo_xFe_{12-x}O_{19}$ powders and various magnetic parameters such as saturation magnetization (Ms), remanence (Mr) and coercivity (Hc). The remanent magnetic field and coercivity decreased with increase in Co^{2+} doping. The saturation magnetization of pure $SrFe_{12}O_{19}$ was lowered due to Cobalt doping. The decrease was more for x=0.3 and with more doping of Co^{2+} in $SrFe_{12}O_{19}$ in place of Fe^{3+}, the saturation magnetization increased but having lesser value than those of pure $SrFe_{12}O_{19}$. As the coercivity of the samples decreased from 4000 Oe to 342 Oe due to increase in cobalt concentration in $SrCo_xFe_{12-x}O_{19}$; the samples with x>1 may show soft ferrite behavior. In ferrimagnetism, two sublattices that align antiparallel to each other result from the difference between the magnetic moments of tetrahedral and octahedral sites. Substituting portion of a divalent in at tetrahedral or octahedral sites would modify the intrinsic magnetic properties of ferrites. The magnetic moment in M-type hexaferrite is due to the distribution of iron on five non-equivalent sublattices as described earlier. Out of these five sites 12k, 2a, and 2b have upward spins and $4f_1$ and $4f_2$ have downward spin of electrons. The total magnetic moment (i.e.,20 μ_B) is due to uncompensated upward spins. The Co^{2+} (4 μ_B) replaces Fe^{3+} ion (5 μ_B) which is responsible for the reduction in saturation magnetization and remanence of the synthesized materials (T. Kikuchi et al.).

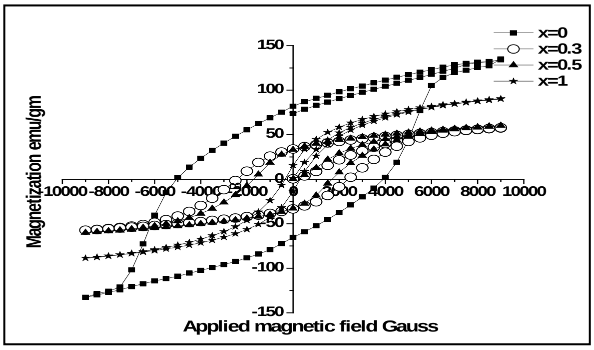

FIG. 6. DC MAGNETIC HYSTERESIS LOOPS FOR $SrCo_xFe_{12-x}O_{19}$ POWDERS

The low value of the coercive field obtained in the present case can be due to lowering of magnetocrystalline anisotropy and/or high degree of aggregation. The magnetocrystalline anisotropy constant for pure strontium hexaferrite is tabulated in table 2. The magnetocrystalline anisotropy constant was decreased due to cobalt doping in $SrFe_{12}O_{19}$ in place of iron and hence, coercivity was reduced after cobalt doping. The dominant contribution to the anisotropy is due to the Fe^{3+} ions located on the 2b sites in the magnetoplumbite structure. Additional contribution comes from the Fe^{3+} ions on the 4f sites. Replacement of the Fe^{3+} ions on these two sites by impurity ions will cause a lowering of the coercivity (H. Luo et al.).

Conclusions

The decrease in c/a ratio and increase in X ray density of pure strontium hexaferrite was obtained due to Co^{2+} doping in place of Fe^{3+} which possibly results from shrinkage of Fe-O bond radii in tetrahedral site. Introduction of Co^{2+} ions in place of Fe^{3+} causes stretching of Me-O bonds and results in the shift in frequencies towards lower value. With increase in substituent concentration, the charge carrier concentration and activation energy of electron hopping increases but the drift mobility decreases. The remanent magnetic field and coercivity decreased with

increase in Co doping in pure $SrFe_{12}O_{19}$ whereas, saturation magnetization of $SrCo_xFe_{12-x}O_{19}$ was decreased upto x=0.3 and then increased. Thus, the DC electrical and magnetic properties of $SrCo_xFe_{12-x}O_{19}$ can be tailored by varying the doping concentration i.e. (x) of cobalt even with insignificant amounts of dopant.

ACKNOWLEDGMENT

One of the authors Dr. Vijaya Puri is gratefully acknowledged to UGC for the award of research scientist 'C' and also thankful to DST, UGC- SAP and DST-PURSE India.

REFERENCES

Chen, N., Yang, K., Gu, M.Y., "Microwave absorption properties of La-substituted M-type strontium ferrites", *J. Alloys Compd.* Vol. 490, pp. 609-612, Feb. 2010.

Elkady, H.A., Abou-Sekkina, M.M., Nagorny, K., "Mössbauer effect and discovery of new hexagonal ferrites prepared at 980°C", *Hyperfine Interactions* Vol. 116, pp. 149-157, Mar. 1998.

Eraky, M.R., "Electrical conductivity of cobalt–titanium substituted SrCaM hexaferrites", *J. Magn. Magn. Mater.* Vol. 324, pp. 1034-1039, March 2012.

Haq, A., Anis-ur-Rehman, M., Malik, M. A., "Structural and electrical transport properties of proficient Ba–Pb nanoferrites", *Phys. Scr.* Vol. 85, pp. 035602-1-035602-6, March 2012.

Iqbal, M. J., Ashiq, M. N., Hernandez-Gomez, P., Munoz, J. M., "Synthesis, physical, magnetic and electrical properties of Al–Ga substituted co-precipitated nanocrystalline strontium hexaferrite", *J. Magn. Magn. Mater.* Vol. 320, pp. 881-886, March 2008.

Iqbal, M. J., Barkat-ul-Ain, "Synthesis and study of physical properties of Zr^{4+}–Co^{2+} co-doped barium hexagonal ferrites", *Mater. Sci. Engg. B.* vol. 164, pp. 6 - 11, Aug. 2009.

Kikuchi, T., Nakamura, T., Yamasaki, T., Nakanishi, M., Fujii, T., Takada, J., Ikeda, Y., "Magnetic properties of La–Co substituted M-type strontium hexaferrites prepared by polymerizable complex method", *J. Magn. Magn. Mater.* Vol. 322, pp. 2381-2385, Aug. 2010.

Luo, H., Rai, B.K., Mishra, S.R., Nguyen, V.V., Liu, J.P., "Physical and magnetic properties of highly aluminum doped strontium ferrite nanoparticles prepared by auto-combustion route", *J. Magn. Magn. Mater.* Vol. 324, pp. 2602-2608, Aug. 2012.

Mallick, K. K., Shepherd, P., Green, R. J., "Magnetic properties of cobalt substituted M-type barium hexaferrite prepared by co-precipitation" *J. Magn. Magn. Mater.* Vol. 312, pp. 418-429, May 2007.

Mathad, S. N., Puri, Vijaya, "Structural and dielectric properties of $Sr_xBa_{1-x}Nb_2O_6$ ferroelectric ceramics", *Arch. Phys. Res.*, Vol. 3 (2), pp. 106-115 May 2012.

Nilpairach, S., Udomkichdaecha, W., Tang, I., "Coercivity of the co-precipitated prepared hexaferrites, $BaFe_{12-2x}Co_xSn_xO_{19}$", *J. Korean Phys. Soc.* Vol. 48 (5), pp. 939-945, May 2006.

Pieper, M. W., Kools, F., Morel, A., "NMR characterization of Co sites in La+Co-doped Sr hexaferrites with enhanced magnetic anisotropy", *Phys. Rev. B* Vol. 65, pp. 184402-1-184402-5 May 2002.

Rao, B.P., Rao, K.H., Sankaranarayana, G., Paduraru, A., Caltun, O.F., "Influence of the V_2O_5 additions on the resistivity and dielectric properties of nickel zinc ferrites", *J. Optoelect. Adv. Mater.* Vol. 7, 697-700, April 2005.

Shaikh, P.A., Kambale, R.C., Rao, A.V., Kolekar, Y.D., "Structural, magnetic and electrical properties of Co–Ni–Mn ferrites synthesized by co-precipitation method", *J. Alloys. Compounds*, Vol. 492, pp. 590-596 March 2010.

Shepherd, P., Mallick, K. K., Green, R. J., "Dielectric properties of cobalt substituted M-type barium hexaferrite prepared by co-precipitation", *J. Mater. Sci.: Mater. Electron.* 18 (5), pp. 527-534, May 2007.

Valenzuela, R., *Magnetic Ceramics*, Cambridge University Press, (2005).

Zhao, W., Wei, P., Cheng, H., Tang, X., Zhang, Q., "FTIR Spectra, Lattice Shrinkage, and Magnetic Properties of CoTi-Substituted M-Type Barium Hexaferrite Nanoparticles", *J. Am. Ceram. Soc.*, Vol. 90 (7), pp. 2095-2103, July 2007.